Contribution of gaseous and particulate species to droplet solute composition

K. Sellegri, Paolo Laj, A. Marinoni, R. Dupuy, Michel Legrand, S. Preunkert

Atmos. Chem. Phys. Discuss., 3, 479–519, 2003
www.atmos-chem-phys.org/acpd/3/479/

Atmospheric Chemistry and Physics Discussions

Contribution of gaseous and particulate species to droplet solute composition

K. Sellegri[1, 3], **P. Laj**[1], **A. Marinoni**[1], **R. Dupuy**[1], **M. Legrand**[2], **and S. Preunkert**[2]

[1]Laboratoire de Meteorologie Physique, CNRS, Université Blaise Pascal, 24, av. des landais, 63177 Aubiere cedex, France
[2]Laboratoire de Glaciologie et Géophysique de l'Environnement, 54, rue Molière, 38402 St. Martin d'Hères cedex, France
[3]now at MPI Heidelberg, Germany

Received: 5 December 2002 – Accepted: 13 January 2003 – Published: 3 February 2003

Correspondence to: K. Sellegri (k.sellegri@mpi-hd.mpg.de)

Abstract

Chemical reactions of dissolved gases in the liquid phase play a key role in atmospheric processes both in the formation of secondary atmospheric compounds and their wet removal rate but also in the regulation of the oxidizing capacity of the troposphere (Lelieveld and Crutzen, 1991). The behaviour of gaseous species and their chemical transformation in clouds are difficult to observe experimentally given the complex nature of clouds.

In this study, we have deployed an experimental set-up to provide an in-situ quantification of phase partitioning and chemical transformation of both organic (CH_3COOH, $HCOOH$, $H_2C_2O_4$) and inorganic (NH_3, HNO_3, SO_2, HCl) species in clouds.

We found that, carboxylic acids, nitrate, and chloride can be considered close to Henry's law equilibrium, within analytical uncertainty and instrumental errors. On another hand, for reduced nitrogen species, dissolution of material from the gas phase is kinetically limited and never reaches the equilibrium predicted by thermodynamics, resulting in significant sub-saturation of the liquid phase. On the contrary, sulfate is supersaturated in the liquid phase, indicating the presence of significant aerosol-derived material transferred through nucleation scavenging.

Upon droplet evaporation, most species, including SO_2, tend to efficiently return back into the gas phase. In that sense, these species contribute to acidification (for carboxylic acids) or neutralization (for NH_3) of the liquid-phase but not totally of the processed aerosols. The only species that appears to be modified in the multiphase system is nitrate. A fraction of at least 10 to 40% of the liquid phase NO_3^- originates from dissolved HNO_3 of which only a fraction evaporates back to the gas phase upon evaporation, resulting in an NO_3^- enrichment of the aerosol phase. In-cloud gas-to-particle transfer of HNO_3 possibly plays a key role in aerosol acidification and in the modification of their hygroscopic properties.

Our study emphasizes the need to account for the in-cloud interaction between particles and gases to provide an adequate modeling of multiphase chemistry systems and

ACPD

3, 479–519, 2003

its impact on the atmospheric aerosol and gas phases.

1. Introduction

The chemical composition of cloud droplets results from chemical and physical processes that include the dynamics of cloud formation, the composition and concentration of the aerosols that served as CCN (nucleation and impaction scavenging), the transfer of volatile species across the air/water interface during the cloud lifetime and the chemical reactions that can take place in the liquid phase. Predicting the chemical properties of cloud drops therefore requires an accurate knowledge of the efficiency by which chemical species are transferred to and transformed in cloud drops under varying environmental conditions. The transfer efficiency to the condensed phase has considerable impact on the lifetime of some chemical substances as well as on oxidant levels in the troposphere (Lelieveld and Crutzen, 1991, Lawrence and Crutzen, 1998). The most efficient mechanisms that control the solute composition and concentration in cloud drops are nucleation scavenging for particles and gas-liquid equilibrium for gases.

Nucleation scavenging of particles is often described by the Koehler theory: an aerosol particle will or will not be activated to a cloud drop according to its diameter and chemical composition and to the supersaturation of water vapour (Pruppacher and Klett, 1997). This theory, however, appears to be limited to properly describe the activation of organic aerosol particles in particular in the presence of either slightly soluble compounds that dissolve at supersaturation lower than 1% or of elevated concentrations of soluble gases that can depress the water vapour pressure on the droplet surface, shifting the activation radius at a given R.H. towards smaller particles (Kulmala et al., 1995). At present, prediction of the number of CN serving as cloud condensation nuclei (CCN) under given supersaturation is therefore highly uncertain. Generally, between 50 and 90% of particle mass is scavenged into cloud drops through nucleation corresponding to 10 to 90% of the particle number. After condensation of water

ACPD
3, 479–519, 2003

onto the particle is initiated, the growth of the cloud droplet at equilibrium results in the large solute concentration that tends to decrease due to diffusional growth after droplet activation (Ogren et al., 1992; Ogren and Charlson, 1992; Flossmann et al., 1998; Flossmann, 1994). Consequently, a large variability of solute concentration in cloud droplets arises from different environmental conditions.

The scavenging of gases is often estimated by considering Henry's law equilibrium existing between the different phases of the system between gas and aqueous phases for both aerosols and cloud droplets (Warneck, 1986; Schwartz, 1986; Lelieveld and Crutzen, 1991). This assumption, however, does not appear to be fully supported by experimental studies in fog and cloud systems. Deviations from theoretical equilibrium of several orders of magnitude have been found for gases such as SO_2, NH_3 or HCOOH, showing either sub- or super-saturation of the liquid phase of clouds (Facchini et al., 1992a; Facchini et al., 1992b; Keene et al., 1995; Laj et al., 1997; Munger et al., 1995; Noone et al., 1991; Rao and Collett, 1995; Richards et al., 1983; Winiwarter et al., 1988; Winiwarter et al., 1994). Such deviations are not easily explained neither by additional equilibrium nor by in-cloud formation of new compounds (Winiwarter et al., 1994), nor by sampling artefact due to long integration time or droplet heterogeneity (Ricci et al., 1998, Pandis and Seinfeld, 1991; Winiwarter et al., 1992). Mass-transfer limitation across the droplet interface (Schwartz, 1986), inadequate description of cloud dynamics (Audiffren et al., 1996) and/or analytical uncertainties may also result in significant deviations from equilibrium. It is therefore important to assess the extent to which the departures observed at different sites represent the actual behaviour of chemical compounds in clouds and to quantify the possible implications of non-equilibrium for the cloud processing of chemical species in the atmosphere. Overall, it is estimated that uncertainty in describing the equilibrium can lead to significant errors in estimating wet deposition of soluble gases (Lawrence and Crutzen, 1998).

Because the rates of chemical transfer from both nucleation scavenging and gas-liquid equilibrium are often known within a large uncertainty, estimating the solute composition and concentration is not straightforward. Moreover, it is also difficult to

ACPD
3, 479–519, 2003

estimate the relative contribution of each process to the resulting solute composition. Knowledge of this information, however, would be very valuable not only to contribute to the understanding of the chemical cycling of key atmospheric species but also to validate multiphase atmospheric models.

In past literature, these two mechanisms are often considered independently from each other to derive estimates of scavenging efficiencies. For example, the gas contribution to droplet concentration is commonly calculated under the assumption that all particulate material is scavenged with similar efficiencies (Krämer et al., 2000; Husain et al., 2000). On the contrary, aerosol particle scavenging efficiencies are calculated by comparing droplet and interstitial aerosol concentrations and assuming negligible contribution of gases in the cloud droplets (Hitzenberger et al., 2000; Kasper-Giebl et al., 1999; Kasper-Giebl et al., 2000; Limbeck and Puxbaum, 2000).

In the present paper, we propose an experimental methodology to de-couple contributions from gaseous and particulate phase to the solute composition and concentration in cloud samples. The methodology is applied to the study of multiphase systems at the observation site of Puy de Dôme (Central France) to estimate the phase partitioning of sulfur, ammonia, nitrate, carboxylic and dicarboxylic acids between gas and condensed phases and discuss the particulate and gaseous contributions to the ionic concentration in cloud droplets.

2. Experimental methodology

2.1. Sampling strategy

Clouds are extremely complex multiphase systems formed by both dissolved and interstitial gases and aerosols. The experimental strategy is based on separate sampling of the different cloud reservoirs coupled with accurate measurements of cloud microphysics. The experimental deployment is similar to that described by Wobrock et al. (2001) and Sellegri et al. (2003b). Here, we will simply recall the characteristics of the

different samplers that are shown in Fig. 1.

Simultaneous sampling with a Counterflow Virtual Impactor (CVI) and a Round Jet Impactor (RJI) allows the separation between interstitial gases and aerosols and the condensed phase.

- The CVI is based on the principle of the inertial sampling of droplets in a counterflow of pure and dry air (Ogren et al., 1985). The size cut of the instrument is evaluated to 4–5 μm by a set of laboratory, in-situ and modeling calibration experiments. A detailed description of the calibration procedures is given by Vocourt (2002). Droplets sampled by the CVI are heated and evaporated into both residual particles and gases originally dissolved in droplets.
- The RJI is a one-stage impactor with a 50% cut-off close to 5 μm (Wobrock et al., 2001). It is therefore complementary to the CVI inlets as it only samples interstitial gases and aerosols.
- The condensed phase can be directly sampled using a one stage Cloud Droplet Impactor (CDI) adapted for high wind speeds, similar to that used by Kruisz et al. (1993) with a 50% cut-off at 7 μm. Contrary to the CVI this sampler collects aerosol particles and dissolved gases together in the liquid (or ice) phase.
- Finally, a Whole Air Inlet (WAI) samples both interstitial and condensed phases. All phases of the multiphase system are sampled into a stainless-steel duct. A windshield that lowers air speed around the air inlet increases the duct sampling efficiency. All parts of the inlet are heated to avoid ice formation when temperatures are near or lower than 0° C. Sampled droplets are gently evaporated maintaining a relative humidity between 40 and 60% in the duct regardless of the outside conditions.

As schematized in Fig. 1, these four sampling devices are clearly complementary and can be used to study partitioning of chemical species between the different reservoirs. For example, summing measurements in the CVI and the RJI directly compares to

measurements performed in the WAI. Similarly, CVI and RJI measurements provide direct access to partitioning of aerosols and gases between interstitial and condensed phases and comparing gas concentrations in WAI and RJI gives access to the amount of dissolved gases.

2.2. Field site and meteorological conditions

Sampling was performed between 8 February and 1 March 2001 at the summit of the Puy de Dôme (1465 m a.s.l.), France. Prevailing western winds allowed for the sampling of oceanic air masses, which had evolved over 250 km of land, and whose characteristics are typical of a free-troposphere site during wintertime. Local contamination at the site is extremely limited in winter, since the access to the station is restricted to authorized personnel. The site, detailed in Wobrock et al. (2001), is part of several measuring networks that provide information on concentrations of several gases as well as on particle levels. It is equipped for meteorological and cloud microphysical measurements.

In this paper, we will report information from five different cloud events. An overview of the measurements of interest to this study is given in Table 1.

2.3. Chemical analyses

Gases were sampled in the total phase (WAI) and the interstitial phase (RJI) with modified versions of the mist chamber (MC) technique (Talbot et al., 1997). Soluble gases are absorbed on mist droplets created by a capillary in a sampling glass vessel. The sampled air was filtered using Teflon 0.2 μm porosity filters before entering the mist chamber. The sampling duration ranged from one to three hours, at flow rates of 10 l/min and 12 l/min for RJI and WAI mist chambers, respectively. The volume of the sampled air was measured with gas volume meters and corrected for the pressure drop. Each sampling system was composed of two separate mist chambers in order to enhance the collection efficiency of each component. Both vessels were filled with

ACPD
3, 479–519, 2003

40 ml of ultra pure water (tandem Millipore Milli-Q – ELGA Maxima system) and new pre-filters were used after each run.

Cloud water was sampled in the CDI with a typical time step of 1 h. Depending on the air temperature, the water was either found in the liquid state on the impacting collector or in the frozen state (after contact freezing of super-cooled droplets). The impactor is made of both aluminum and stainless steel. All parts of the impactor in contact with the samples were cleaned by repeated immersion and sonication in MilliQ water. The sampled water was transferred either directly or after short melting into 250 ml glass vials cleaned with similar procedures as described above. All manipulations were performed under a horizontal laminar flow bench equipped with an additional activated charcoal filter to limit interaction of substrates with HNO_3 or NH_3 vapors possibly present in the room.

A Gerber probe PVM-100 installed in a wind tunnel at the station measured the liquid water content of the cloud. Previous measurements showed that LWC is measured with a precision of about 20%.

Aerosol particles were sampled in the CVI using a 12-stage low-pressure cascade impactor (SDI 11 l/min), with cut size diameters of 0.045, 0.086, 0.153, 0.231, 0.343, 0.591, 0.796, 1.060, 1.66, 2.68, 4.08, 8.39 μm. The sampling time resolution was typically 20 h. Zhang et al. (1992) studied the artifacts due to the volatilization of nitrate in the instrument and concluded that it is significantly lower than when sampling with filters. Concerning nitrate, a high gas-to-particle ratio increases losses, and they are expected to be significant for ratios ranging from 1.0 to 10.0. As gases are excluded during sampling with the CVI, this artifact can be definitely excluded. Polycarbonate filters (0.2 μm pore size) were used as impaction substrates. They were not coated in order to eliminate analytical complexities associated with the use of grease. Bouncing of particles from one stage to another is limited due to the low concentration of particles (especially in the super-micronic range) and the sampling RH maintained between 40 and 60%. Impactor loading and unloading was performed in the field inside the horizontal laminar flow bench. Samples are stored in individual tight Petri dishes

ACPD
3, 479–519, 2003

(Analyslides®) and kept frozen until analysis. Blank samples were performed on a regular basis by loading the impactors in the field and performing extraction and chemical analyses similar to those performed for regular samples. The mass concentration of particles was calculated by summing all impactor stages.

All liquid (CDI and MC) samples and impaction substrates were frozen until analysis, which is usually performed no more than a few days after sampling. Filter extraction and ion chromatography analyses were performed inside a Class 1000 clean room to prevent from external contamination. Polycarbonate filters were extracted in ultrapure water by 15 min soaking, while MC and CDI samples already in the water phase did not undergo any pretreatment before analysis. All samples are analyzed by Ion Chromatography using a DIONEX 100 chromatograph, equipped with a CS12 column for cations, and with a DIONEX 500 chromatograph, column AS11 for anions. Analyzed species of interest are CH_3COO^-, $HCOO^-$, Cl^-, NO_3^-, SO_4^{2-}, Ox^- ($C_2O_4^-$), Na^+ and NH_4^+. Other ions are also analyzed in order to drive the H^+ concentration from the ionic balance. Further details on the analytical procedure are given by Jaffrezo et al. (1998). The precision of the analytical method is evaluated to 10% for samples ten times the detection limit and around 50% for samples less than two times the detection limit. Atmospheric detection limits per impactor stage are derived from the analysis of blank values and defined as mean blank plus standard deviation on blank, for an arbitrary sampling volume of 25 m^3 for impactor data, for a typical 0.3 g/m^3 LWC for CDI data; and for a typical one hour long sampling time for MC data (Table 2).

3. Measurement uncertainties

Because the methodology is based on comparing different instrumentation connected to different inlets, it is important to discuss the possible sampling artifacts and errors.

First, slight differences exist between the cut-off size of the various samplers (5 μm for CVI and 7 μm for CDI), thus an underestimation of the liquid-phase concentration can arise in the CDI due to the fact that small droplets are generally more concentrated

ACPD
3, 479–519, 2003

than larger ones (Laj et al., 1998; Schell et al., 1997). On average, in a typical cloud droplet spectrum at puy de Dome, the water mass comprised between 5 and 7 μm is lower than 5% of the total mass. Under these conditions, and assuming that smaller droplets ($< 7\,\mu$m) are 20% more concentrated than larger ones (Schell et al., 1997), this would lead to a difference in concentration of the order of 6%.

Second, the liquid-phase concentrations are corrected for the LWC to be compared to the other cloud reservoirs. We have used an average LWC value over the sampling duration. The LWC, however, varies during the course of a cloud event. Moreover, high LWC values are generally linked to increased small droplet concentrations, which are not efficiently sampled in the CDI. This will lead to an overestimation of the liquid phase concentration after conversion to atmospheric concentration (nmol m^{-3}).

Third, the cloud LWC is known with an accuracy of about 20% resulting in a large uncertainty in the atmospheric concentrations of the liquid phase.

Fourth, an additional source of errors arises from contact freezing of super-cooled cloud samples and unknown retention coefficients between liquid and ice phases. This point is discussed later in the paper.

Finally, comparison of instrumentation is often difficult especially when their conception differs fundamentally. Based on these considerations, it should be kept in mind that large measurement errors are associated to some of our results, in addition to analytical uncertainties. To overcome this problem, we often based the discussion on relative rather than absolute differences. In fact, because our results tend to show very consistent figures for the different cloud events, atmospheric processes can successfully be studied with this methodology. In addition, some of our measurements are in theory redundant, thus whenever possible, comparisons between similar instrumentation is preferred over comparisons between different instrumentation.

4. Results

4.1. Chemical composition of the liquid phase

SO_4^{2-}, NH_4^+, and NO_3^- account for more than 80% of the total analyzed anions while chloride and carboxylic acids account for 8 and 9 %, respectively. The contribution of organic acids is low compared to the major ions and never exceeds a few percent of the total mass. Sulfate concentrations range from 4 to 40 μmol l-1, which is very similar to levels found in clouds at most of the European altitude sites: between 27 to 70 μmol l^{-1} measured at Mt Sonnblick (Hitzenberger et al., 2000), Mt Jungfraujoch (Baltensperger et al., 1998) and Kleiner Feldberg (Wobrock et al., 1994). The maximum values are an order of magnitude lower than concentrations measured at Puy de Dôme during the CIME 1998 experiment and at Great Dun Fell, (360 and 240 μmol l^{-1}, respectively, Laj et al., 2001; Laj et al., 1997). Similar considerations can be made for NH_4^+ and NO_3^- concentrations (28-150 μmol l^{-1} and 12-93 μmol l^{-1}, respectively), comparable to the concentrations measured at Kleiner Feldberg (180 μmol l^{-1} for both species; Wobrock et al., 1994), but an order of magnitude higher than those measured at Jungfraujoch (16 and 10 μmol l^{-1}; Baltensperger et al., 1998), and an order of magnitude lower than the those measured at the Puy de Dôme or Great Dun Fell (90–2000 μmol l^{-1} for NH_4^+ and 5–1000 μmol l^{-1} for NO_3^-; Laj et al., 2001; Laj et al., 1997).

The liquid-phase concentrations can be converted to atmospheric concentrations using an integrated value of LWC over the sampling duration. This makes comparison with other cloud reservoirs much easier. Concentrations, after conversion to nmol m^{-3}, are presented in Table 3 for each cloud event. This leads to extremely variable atmospheric concentrations due to changing LWC. The chemical composition of cloud droplets does not undergo significant variation during the course of a cloud event while atmospheric concentrations of the dissolved species can vary up to a factor of 20. Overall, concentrations of SO_4^{2-}, NH_4^+ and NO_3^- vary from 1.1 to 20 nmol m^{-3}, 7.4 to 62.5 nmol m^{-3} and 4 to 86 nmol m^{-3}, respectively. The concentrations of acetic and

ACPD
3, 479–519, 2003

formic acids are both ranging from 1 to 2.2 nmol m^{-3} while that of oxalate is lower (0.13 to 0.65 nmol m^{-3}).

Most samples are slightly acidic with a median cation/anion equivalent ratio of 0.88 ± 0.16, as expected from previous measurements at PDD (Flossmann et al., 2000). The $NH_4^+/(SO_4^{2-} + NO_3^-)$ ratio decreases with increasing acidity confirming that sulfate and nitrate play a substantial role in the acidification process. The NO_3^-/SO_4^{2-} molar ratio ranges from 0.6 to 1.1 that is lower than that reported by Fuzzi et al. (1994) for the Kleiner Feldberg (molar ratio of the order of 0.5–1.5). Two samples, corresponding to two fractions of the same cloud event, are basic as a result of NH_4^+ increase. The Cl^-/Na^+ ratio is 80% higher than the sea-salt ratio indicating a clear Cl^- enrichment, likely from gaseous HCl incorporation in the liquid phase.

As mentioned earlier, most samples are collected during freezing conditions. Upon freezing, a fraction of the gas dissolved in the super-cooled droplets is transferred back to the gas phase while another is retained in the ice matrix. The retention coefficient is defined as the fraction remaining in the ice. There is still a lot of uncertainty on the retention coefficient even for the most common atmospheric gases. A low retention coefficient would lead to an underestimation of the gaseous concentrations in super-cooled water. However, the retention coefficient observed by Voisin et al. (2000) for HNO_3, HCl and NH_3 is close to 1. This is confirmed by the fact that samples collected during warm events do not show higher condensed-to-gas phase ratios than the other samples. We do not have any information on retention coefficients for organic acids.

4.2. Composition of particulate droplet residuals

The chemical composition of droplet particulate residuals measured during the five cloud events is given in Table 4. Because the chemical and physical properties of the aerosol at Puy de Dôme are discussed in details in Sellegri et al. (2003a), we will here restrict the discussion to issues related to multiphase chemistry of clouds.

As expected, most of the mass (>90%) consists of NH_4^+, SO_4^{2-}, and NO_3^-. The

contribution of carboxylic ions is lower than 2% of the total ionic mass while that of Cl^- is less than 5%. The Cl^-/Na^+ ratio in the droplet residuals is lower than the sea-salt ratio as opposed to the liquid phase, indicating a Cl^- loss corresponding to up to 79% of the expected marine concentration. This confirms that most of the Cl^- originally in the liquid phase volatilizes back to the gas phase upon droplet evaporation. As for Cl^- and organic acids, the contribution of NO_3^- with respect to SO_4^{2-} is often proportionally higher in the liquid phase than in the residual particles, showing significant contribution of the gas phase. The NO_3^-/SO_4^{2-} ratio ranges from 0.4 to 1, and is either equal or half the ratio in the liquid phase, depending on the event. This possibly indicates a higher contribution of NO_3^- to the liquid phase compared to SO_4^{2-}. As a result, NO_3^- is in the liquid phase the most concentrated ion by mass. Note that this is not usually the case for bulk (interstitial + residual) aerosols in the absence of clouds for which SO_4^{2-} is the predominant ion (Sellegri et al., 2003b). On the contrary, the oxalate/SO_4^{2-} and NH_4^+/SO_4^{2-} ratios are similar in both liquid and residual phases.

4.3. Composition of the interstitial gaseous phase

Because sampling is performed in clouds, the presence of gas molecules in the interstitial air results from both their original concentration before cloud formation and their ability to dissolve in cloud droplets. The concentrations of the main inorganic gases (SO_2, HNO_3, HCl and NH_3) as well as HCOOH, CH_3COOH and $C_2O_4H_2$ acids in the interstitial phase of clouds are summarized in Table 5. The concentrations are dominated by NH_3 (18–52 nmol m^{-3}), HCOOH (2.8–7 nmol m^{-3}), and CH_3COOH (6–17 nmol m^{-3}) while concentrations of HCl, SO_2, HNO_3, $C_2O_4H_2$ never exceed 20 nmol m^{-3} but for HCl in one sample, and are often below detection limits. This is similar to other measurements performed in clouds showing reduced interstitial concentrations of HNO_3 and higher concentrations of organic acids (Facchini et al., 1992a; Fuzzi et al., 1994). Also, the interstitial concentration of NH_3 is variable depending on the intensity of the agricultural source (Facchini et al., 1992a; Fuzzi et al., 1994).

ACPD
3, 479–519, 2003

Voisin et al. (2000) performed similar measurements at Puy de Dôme by during the winter 1998 (CIME experiment) using the MC technique. Concentrations are in the same range for HCOOH, CH_3COOH and HCl. However, our measurements show much higher concentrations of NH_3 and lower for HNO_3 and SO_2.

4.4. Composition of the interstitial aerosol phase

Interstitial aerosol particles are mostly composed of the major ions SO_4^{2-}, NO_3^- and NH_4^+, but their concentrations are one order of magnitude lower than in the residual phase (Table 6), indicating efficient nucleation scavenging (Sellegri et al., 2003b). Concentrations of organic acids are very often below detection limits and those of Cl^- do not get higher than 0.4 nmol m^{-3}. In addition to the reduced mass of inorganic compounds left in the interstitial phase, there is a clear depletion of NO_3^- compared to residual and liquid phases. This can be seen comparing NO_3^-/SO_4^{2-} and NH_4^+/NO_3^- ratios in interstitial, residual and liquid phases. As for clear-sky aerosols, SO_4^{2-} is the most concentrated ion in the interstitial and the NO_3^-/SO_4^{2-} ratio is lower or equal to 0.6 showing a higher relative NO_3^- content in residual particles compared to non-incorporated particles, as respect to other inorganic species. On the contrary, no clear difference is measured between the proportions of NH_4^+ and SO_4^{2-} in interstitial and residual phases.

5. Discussion: behavior of chemical species in the multiphase system

5.1. Gas/liquid partitioning

The mass partitioning of a chemical compound X between interstitial gaseous phase and condensed phases (R_x) can be expressed as:

$$R_x = 100^*[X]_{liq}/([X]_{liq} + [X]_{int,\,gas}). \quad (1)$$

ACPD
3, 479–519, 2003

Where liq refers to the liquid phase, int to the interstitial phase and all concentrations are in nmol m-3. R_x, therefore, is the mass fraction (in %) of the compound in the liquid phase. The interstitial-phase concentration is the sum of both the gaseous and particulate phases. However, the interstitial particles never exceed more than 14% of the total inorganic species. In the following, this contribution is neglected and we have used the gaseous phase concentration ($[X]_{gas}$) as the interstitial concentration in Eq. (1). $[X]_{gas}$ is the concentration of the species X in the gas phase from the mist chamber measurement in the RJI while $[X]_{liq}$ is the concentration of the species X in the liquid phase collected in the CDI. Percent mass fractions R_x of the different analyzed species are summarized in Table 8 for the 5 cloud events.

Chloride, nitrate, sulfate and oxalate are predominantly in the condensed phase while acetate, formiate, and NH_3 are in the interstitial phase. It is interesting to note that very little variation is found among the different cloud events. These results are similar to those observed by Voisin et al. (2000) for carboxylic acids, chloride and nitrate. On the contrary, in our study, about 62% of NH_3/NH_4^+ is present as NH_3. That is higher than what was found by Voisin et al. (2000) and Kasper and Puxbaum (1998) but similar to measurements of Laj et al. (2001) at PDD. The partitioning of sulfur species is clearly shifted towards the condensed phase (75% to 100% of the mass is present in the liquid phase). Such an enrichment of the liquid phase is neither found by Fuzzi et al. (1994), nor by Facchini et al. (1992a) who rather found a high gas-phase contribution. The reason for this feature could lay in the fact that the SO_2 concentrations are much higher at Kleiner Feldberg and Po Valley where these latter studies were performed, than at Puy de Dôme.

It is possible to investigate whether the measured partitioning corresponds to that predicted by Henry's law equilibrium. We have taken the following reactions into consideration (Table 7). All enthalpies and equilibrium constants are corrected for temperature effects according to Van't Hoff equation, taking pH into consideration (except for oxalic acid for which the reaction enthalpy is not available in the current literature). The theoretical R_x are summarized in Table 8. As mentioned, this calculation accounts for

the dissolution of species in the liquid phase and formally leads to an effective Henry's law constant.

The theoretical and measured R_{Cl}, R_{NO3}, and R_{ox} are close to 100%, showing that most of the mass lies in the liquid phase. According to this calculation, all three species can, therefore, be considered at Henry's law equilibrium, within analytical uncertainty and instrumental errors. This result is especially interesting for oxalic acid since it is the first experimental determination of its phase partitioning in clouds. Concerning monocarboxylic acids, it is difficult to tell whether the liquid phase is subsaturated or not, regarding the uncertainties assiciated to each (calculated and measured) value.

However, NH_4^+ exhibits a clear deficit in the liquid phase as compared to theoretical values. Such subsaturation of the liquid phase was already observed by Voisin et al. (2000). As for this study and those of Laj et al. (1997) and Winiwarter et al. (1994), the subsaturation increases with increasing pH. The subsaturation of the liquid phase is likely resulting from mass transfer limitation between gaseous and liquid phase as proposed by Ricci et al. (1998) and Winiwarter et al. (1994).

On the other hand, SO_4^{2-} is supersaturated in the liquid phase showing between 75 and 100% of the sulfur species in the liquid phase as opposed to the expected 0.1 to 15%. Obviously, the theoretical partitioning is calculated for S^{IV} species (HSO_3^- + SO_3^{2-}) while SO_4^{2-} is analyzed and used in the experimental partitioning. The implicit assumption is that all S^{IV} is oxidized to S^{VI} in the liquid samples awaiting or during chemical analysis. Because the liquid phase is analyzed several hours after sampling and despite the fact that samples are kept frozen, oxidation can proceed either via reaction with O_3 or H_2O_2 resulting in complete S^{IV} oxidation. This is confirmed by the absence of SO_3^- traces in the samples and previous comparison between artificially oxidized and non oxidized mist chamber samples (Voisin et al., 2000). If some S^{IV} is still present in the liquid phase (that is unlikely), the liquid concentrations would be underestimated. Thus the supersaturation of sulfate in the liquid phase is not resulting from a sampling artifact. The apparent super-saturation of the liquid phase can be explained by the high amount of particulate transferred to the liquid phase by nucleation

scavenging (Ricci et al., 1998). A fraction of the solute concentration of almost all chemical species originates, in fact, from the particulate phase. The pH dependence of the supersaturation shown by several authors (Winiwarter et al., 1994; Ricci et al., 1998; Laj et al., 1997) is clearly an artifact resulting from the fact that transfer through nucleation scavenging is not pH dependent.

5.2. Degassing efficiencies upon droplet evaporation

Chemical reactions of dissolved gases in the liquid phase play a key role in atmospheric process both for the formation of secondary compounds but also for their impact on gas-phase chemistry. In-cloud chemical reactions tend to increase the oxidation state, often leading to irreversible formation of new compounds. The newly formed compounds have different physico-chemical properties and their fate upon droplet evaporation may differ from that of the original reduced compound. This is the case for gaseous SO_2 oxidation that is considered a major source of particulate S(VI). It is therefore interesting to investigate the behavior of the gas-derived fraction of cloud droplets upon evaporation.

Significant amounts of SO_2, HNO_3, HCOOH, HCHO and H_2O_2 evaporating from cloud droplets have been measured directly behind a CVI inlet (Flossmann, 1998; Laj et al., 2001; Noone et al., 1991). Cape et al. (1997) estimated that as much as 25% of the cloud nitrate could be released as HNO_3 as cloud droplets evaporated. This is lower than a calculation by Laj et al. (1998) estimating that 60 to 80% of the dissolved HNO_3 and NH_3 is degassing from droplets upon evaporation. Overall, in-cloud chemical reactions only transform a fraction of the dissolved species.

With our experimental set-up, it is possible to estimate the gas fraction that has evaporated from the droplet solute concentration, which is the fraction that did not undergo irreversible transformation. This is done by calculating the particulate mass concentration difference between CDI (gases + scavenged aerosols) and CVI (scavenged aerosols only). This can be computed in other ways but we avoided comparing absolute CDI to absolute mist chamber concentrations as that would lead to an uncertainty

higher than 100%, especially for low-concentrated samples. Therefore, calculation is performed in the following way (C_{Xgas} is the mass fraction of a given species X that degassed from the droplet solution):

$$C_{Xgas} = 1 - ([X]_{CVI}/[X]_{CDI}) \quad (2a)$$

or

$$C_{Xgas} = 1 - ([X]_{part}(\text{nmol m}^{-3})/([X]_{water}(\text{nmol/l})^{*}\text{LWC}(\text{g m}^{-3})^{*}\rho_{eau}(\text{g.l}^{-1}))). \quad (2b)$$

Where [X]part derives from the cascade impactors data and [X]water derives from the CDI data. The liquid-water sampling with CDI is performed with a typical time resolution of 1 h while the particle sampling with cascade impactor is performed per event (typically 20 h time resolution). Consequently, several runs of CDI samples are averaged to compare particulate to liquid concentrations.

This calculation is based on subtraction and division of concentrations in the different cloud reservoirs. In order to avoid making comparisons between absolute concentrations in the different cloud reservoirs, we can also work with relative concentrations referred to a given species. In that case, we have chosen Na^+ as a reference species based on the hypothesis that sodium is conservative and is not present in the gas phase ($[Na^+]_{part} = [Na^+]_{water}$). Then, C_{Xgas} can be expressed as:

$$C_{Xgas} = 1 - ([X]_{CVI}/[Na^+]_{CVI})/([X]_{CDI}/[Na^+]_{CDI}) \quad (3a)$$

or

$$C_{Xgas} = 1 - ([X]_{part}/[Na^+]_{part})/([X]_{water}/[Na^+]_{water}). \quad (3b)$$

This calculation method also avoids converting liquid concentrations to atmospheric concentrations and thus limits the artifacts associated to the integration of LWC over the CVI sampling period. The contribution of the gaseous phase to the droplet solute concentration calculated using both relative and absolute concentrations only differs

ACPD
3, 479–519, 2003

within analytical uncertainties. Results are presented in Fig. 2 where C_X = 100% corresponds to a complete degassing from droplets. The degassing is extremely variable among gases, ranging from 10 to 100%.

It is clear that the degassing of acetic and formic acids is quite efficient, as it appears to account for almost all dissolved material. The limited amount of carboxylic acids that dissolves in droplets is readily evaporated back to the gas phase upon cloud disappearance. However, we cannot exclude in-cloud production of carboxylic acids.

Chloride shows the highest degassing efficiency of all inorganic species with more than 85% (and up to 95%) of the solute concentration being released as HCl during droplet evaporation. Such an efficient degassing leads to significant chloride depletion in solid residues, up to 80% of the expected sea salt chloride. Although it is difficult to quantify the in-cloud conversion of particulate Cl^- to HCl in our experimental set-up, the cloud reactor potentially favours the chloride depletion that is often encountered in the aerosol phase.

The presence of a high-degassed fraction of dissolved $C_2O_4^{2-}$ is more surprising as this chemical species is rarely found in the gas phase. The presence of $C_2O_4^{2-}$ in the liquid phase can be due to its production from another dissolved gas than $H_2C_2O_4$, or from other particulate carbonaceous species. The absence of $H_2C_2O_4$ in the interstitial gas phase and in the gases evaporated from the droplets can be due to difficulties in sampling this compound because of its low solubility. More work is necessary on that issue but it seems clear that not all oxalic acid present in the liquid phase is found as a particulate residue.

Again, as for carboxylic acids, a large fraction of dissolved NH_3 returns back to the gas phase upon evaporation. The amount of degassed NH_3 accounts for 50–60% of the dissolved fraction. This is surprising, considering the fact that residual aerosols are acidic, and the liquid phase is subsaturated. The NH_4^+/SO_4^{2-} equivalent ratio is very similar in the liquid and solid residual phases leading to the conclusion that these species are evaporated out of the droplet with the same efficiency. The fraction of S^{IV} that is converted to S^{VI} in cloud retains NH_4^+ upon evaporation of the droplet leading to

ACPD
3, 479–519, 2003

$(NH_4)_2SO_4$ formation in the droplet residual.

Between 20 and 40% of SO_4^{2-} present in the liquid phase degasses upon droplet evaporation. This is relatively high considering the importance of the particulate phase and indicates that the amount of SO_2 converted to SO_4^{2-} is limited. Only one sample (sample 2) shows reduced degassing of SO_2 due to potential SO_2 oxidation. This sample is clearly influenced by anthropogenic activities as shown by the elevated concentrations of sulfate, nitrate, ammonium and carboxylic acids and the low pH. Unfortunately, we do not have an indication on H_2O_2 levels to understand what favored S(VI) formation.

The degassing fraction of NO_3^-, ranging from 10 to 60%, corresponds to that calculated for sulfur degassing as SO_2. Because NO_3^- is more concentrated than SO_4^{2-} in the liquid phase, a similar degassing efficiency leads to enrichment of NO_3^- in the particulate phase relative to SO_4^{2-}. As mentioned earlier, the liquid and residual phases are enriched in NO_3^- with respect to the interstitial phase. At the Puy de Dôme, processing of aerosols mostly deals with gas-to-particle conversion of HNO_3 rather than oxidation of SIV to SVI. Consequently, HNO_3 would not only contribute to acidification of the cloud droplets but also of the residual aerosols.

5.3. Gaseous and particulate contributions to droplet concentration

Overall, taking into account results from Tables 3–6 and the previous calculation, we can propose a global view of the partitioning of $HCOOH/HCOO^-$, CH_3COOH/CH_3COO^-, HCl/Cl^-, HNO_3/NO_3^-, SO_2/SO_4^{2-}, $H_2C_2O_4/C_2O_4^{2-}$ and NH_3/NH_4^+ in clouds, including the contribution of the gaseous and particulate phases to the solute concentration (Fig. 3). In order to evaluate the gas contribution of species to the cloud droplet composition, we assume that gases incorporated in clouds are degassing upon droplet evaporation (and calculated as in Eqs. 2a or 2b). Thus, calculated gas contributions are lower limits, because oxidation in the liquid phase previous to evaporation cannot be evaluated. In Fig. 3, the contributions are averaged over the 5 cloud events.

ACPD
3, 479–519, 2003

The major fractions of CH_3COOH/CH_3COO^- and $HCOOH/HCOO^-$ are in the gas phase and not in the liquid phase. Moreover, most of the carboxylic acids present in the liquid phase are essentially originating form the gas phase and the apparent subsaturation is due to incomplete dissolution due to mass transfer limitation. Assuming Henry's law equilibrium therefore leads to a significant overestimation of the wet deposition of both organic acids. No consumption in the liquid phase seems to take place unless a significant production occurs simultaneously, which is unlikely.

A large fraction (67%) of reduced nitrogen also lies in the interstitial gaseous phase contrary to thermodynamic predictions. Elevated concentrations of interstitial NH_3 were also measured by Laj and coworkers (2001) using completely different techniques. Its presence is explained by extended agricultural areas around the Puy de Dôme. This leads to a clear deviation from Henry's law equilibrium with subsaturation of the liquid phase. Considering that only half of NH_4^+ in the liquid phase originates from the gas phase, the gas-phase transfer deficiency is even higher. Contrary to the conditions encountered in the Po Valley fog (Ricci et al., 1998), particulate ammonium does not compensate for dissolved NH_3 to reach equilibrium. Gaseous NH_3 therefore plays a key role in neutralizing cloud droplets at Puy de Dôme. Assuming Henry's law equilibrium would again overestimate wet deposition.

All other inorganic species are mostly found in the condensed phase with an interstitial gas fraction of the total mass smaller than 11%. The origin of the liquid phase fraction varies depending on the chemical compound. The contribution from gas phase is predominant for Cl^- (74%). It appears from the size distributions of chloride in the residual particles (Sellegri et al., 2003b) that cloud processing does not tend to redistribute Cl^- to droplet residues (i.e. cloud processed aerosol) of all sizes.

The contribution from the particulate phase is higher for SO_4^{2-} and NO_3^- (45%). This is not surprising given their elevated concentration in the particulate phase, that could limit the gas dissolution. In fact, measurements of degassing HNO_3 with mist chambers in the WAI also showed that no HNO_3 degasses. However, recent studies have questioned the use of mist chambers for the determination of HNO_3 and HCl concentrations

due to their ability to stick to tubing and glassware (Neuman et al., 1999). Similarly, the comparison of MC and denuders by Voisin et al. (2000) shows a reasonable agreement for all species except HNO_3 which was two times higher in the denuder tubes than in the MC. Consequently, the interstitial gas fraction presented in this paper might be underestimated, from being sampled with mist chambers. The gas fractions of the total mass are thus lower limits for these two species. The gas/particulate contributions to the liquid concentration should be more reliable, as they are calculated from the CVI and CDI data.

6. Conclusions

The study of the behavior of several key atmospheric compounds was performed using complementary sampling inlets, in the interstitial, residual and liquid phases of a multiphase system. This sampling methodology allowed to de-convolute the behavior of both particulate and gaseous phases of $HCOOH/HCOO^-$, CH_3COOH/CH_3COO^-, $SO_2/HSO_3^-/SO_4^{2-}$, NH_3/NH_4^+, HNO_3/NO_3^- and $H_2C_2O_4/C_2O_4^{2-}$ systems. Overall, we found that the gas contribution to the droplet solute concentration ranges from 30 to 100% depending on the chemical species. This is particularly important considering that aerosol scavenging efficiencies are often calculated assuming a negligible gas-phase contribution to the solute concentration. This can lead to significant overestimation of nucleation scavenging especially for carboxylic acids.

Dissolution of material from the gas phase is kinetically limited and never reaches the equilibrium predicted by thermodynamics, resulting in significant subsaturation of the liquid phase. Thus, monocarboxylic acids and reduced nitrogen species are preferentially found in the interstitial gas phase of clouds despite their high solubility. Only the presence of significant aerosol-derived material transferred through nucleation scavenging can, to some extent, compensate the liquid-phase subsaturation. For all studied species, except monocarboxylic acids and HCl, the degassing efficiencies are below 60% of the concentration in the liquid phase. This indicates that a large fraction of the

dissolved material originates from the aerosol phase, or is produced in the cloud.

If aerosol-derived material is not accounted for in the calculation of Henry's law equilibrium, an effective gas/liquid partitioning corrected for the particulate contribution can be computed that refers to gases only. In that case, the fraction of gaseous compounds dissolved in droplets is 10% for CH_3COOH, 20% for HCOOH, 25% for NH_3, 85% for HNO_3, and 95% for HCl, SO_2, and $H_2C_2O_4$. These values are on average 5% lower than those calculated accounting for dissolved particles, except for NH_3 for which only 25% is found in the liquid phase, as respect to 37% when particulate NH_4^+ is accounted for.

We found almost no evidence of liquid phase reactions of monocarboxylic acids or HCl. Upon droplet evaporation, most species tend to efficiently return back to the gas phase. In fact acetic and formic acids are not found in particulate droplet residues. In that sense, these species contribute to acidification of the liquid phase but do not have a major impact on cloud-processed aerosols.

A fraction ranging from 20 to 60% of NH_4^+ and SO_4^{2-} originally in the liquid phase seems to potentially degas upon evaporation. Given the importance of aerosol-derived material for SO_4^{2-}, this indicates low S^{IV} conversion to S^{VI}. This is certainly due to limited oxidant levels in the wintertime. The stable NH_4^+/ SO_4^{2-} equivalent ratio in the liquid and residual phases indicates that any S^{IV}-to-S^{VI} conversion is paralleled by NH_3 conversion to NH_4^+ upon evaporation, leading to $(NH_4)_2SO_4$ formation in the processed aerosol.

Nitrate appears to be modified in the multiphase system. A fraction of at least 10 to 40% of liquid-phase NO_3^- originates from dissolved HNO_3. This is less than expected from Henry's law equilibrium. Interestingly, only a fraction of the dissolved HNO_3 seems to evaporate back to the gas phase, resulting in a NO_3^- enrichment of the aerosol phase. This confirms independent measurements of Sellegri et al. (2003b) performed at the same site showing droplet particulate residuals enriched in NO_3^-. In-cloud gas-to-particle transfer of HNO_3 possibly plays a key role in aerosol acidification and in the modification of their hygroscopic properties.

ACPD
3, 479–519, 2003

Acknowledgement. This work was supported by CNRS-INSU under the National Program for Atmospheric Research (PNCA) and by the Ministère de la Recherche under ACI-Jeune Chercheur to PL.

References

Audiffren, N., Buisson, E., and Chaumerliac, N.: Deviations from Henry's law equilibrium for chemical species in a polydisperse cloud: The oxidizing capacity of the troposphere, Venice, European Commission, 1996.

Baltensperger, U., Schwikowski, M., Jost, D. T., Nyeki, S., Gäggeler, H. W., and Poulida, O.: Scavenging of atmospheric constituents in mixed phase clouds at the high-alpine site Jungfraujoch Part I: Basic concept and aerosol scavenging by clouds, Atm. Env. 32(23), 3975–3983, 1998.

Cape, J. N., Hargreaves, K. L., Storeton-West, R. L., Jones, B., Davies, T., Colvile, R. N., Gallagher, M. W., Choularton, T. W., Pahl, S., Berner, A., Kruisz, C., Bizjak, M., Laj, P., Facchini, M. C., Fuzzi, S., Arends, B. G., Acker, K., Wieprecht, W., Harrison, R. M., and Peak, J. D.: The budget of oxidized nitrogen species in orographic clouds, Atm. Env., 31, 16, 2625–2636, 1997.

Chameides, W. L.: The photochemistry of a remote marine stratiform cloud, J. Geophys. Res., 89, 4739–4755, 1984.

Facchini, M. C., Fuzzi, S., Kessel, M., Wobrock, W., Jaeschke, W., Arends, B. G., Möls, J. J., Berner, A., Solly, I., Kruisz, C., Reischl, G., Pahl, S., Hallberg, A., Ogren, J. A., Fierlinger-Oberlinninger, H., Marzorati, A., and Schell, D.: The chemistry of sulfur and nitrogen species in a fog system. A multiphase approach, Tellus, 44B, 505–521, 1992a.

Facchini, M. C., Fuzzi, S., Lind, J. A., Kessel, M., Fierlinger-Oberlinninger, H., Kalina, M., Puxbaum, H., Winiwarter, W., Arends, B. G., Wobrock, W., Jaeschke, W., Berner, A., and Kruisz, C.: Phase partitioning and chemical reactions of low molecular weight organic compounds in fog, Tellus, 44B, 533–544, 1992b.

Flossmann, A. I.: A 2-D spectral model simulation of the scavenging of geaseous and particulate sulfate by a warm marine cloud, Atm. Res., 32, 233–248, 1994.

Flossmann, A. I.: Interaction of aerosol particles and clouds, J. Atmos. Sciences, 55, 879–887, 1998.

Flossmann, A.: Cloud Ice Mountain Experiment (CIME) Final Report, Aubière, France, Laboratoire de Météorologie Physique, 2000.
Fuzzi, S., Facchini, M. C., Schell, D., Wobrock, W., Winkler, P., Arends, B. G., Kessel, M., Möls, J. J., Pahl, S., Schneider, T., Berner, A., Solly, I., Kruisz, C., Kalina, M., Fierlinger, H., Hallberg, A., Vitali, P., Santoli, L., and Tigli, G.: Multiphase chemistry and acidity of clouds at Kleiner Feldberg, J. Atmos. Chem., 19, 87–106, 1994.
Graedel, T. E. and Goldberg, E. D.: Kinetic studies of raindrop chemistry. 1. Inorganic and organic processes, J. Geophys. Res., 88, 865–882, 1983.
Hitzenberger, R., Berner, A., Kromp, R., Kasper-Giebl, A., Limbeck, A., Tscherwenka, W., and Puxbaum, H.: Black carbon and other species at a high-elevation European site (Mount Sonnblick, 3106 m, Austria): Concentrations and scavenging efficiencies, J. Geophys. Res., 105, D20, 24,637–24,645, 2000.
Husain, L., Rattigan, O. V., Dutkiewicz, V. A., Das, M., Judd, C. D., Khan, A. R., Richter, R., Balasubramanian, R., Swami, K., and Walcek, C. J.: Case studies of the SO_2+H_2O_2 reaction in clouds, J. Geophys. Res., 105, D8, 9831–9841, 2000.
Jacob, D. J.: Chemistry of OH in remote clouds and its role in the production of formic acid and peroxymonosulfate, J. Geophys. Res., 91D, 9807–9826, 1986.
Jaffrezo, J.-L., Calas, N., and Bouchet, M.: Carboxylic acid measurements with ionic chromatography, Atm. Env., 32, 2705–2708, 1998.
Kasper, A. and Puxbaum, H.: Seasonal variation of SO_2, HNO_3, NH_3, and selected aerosol components at sonnblick (3106 m a.s.l.), Atm. Env. 32, 23, 3925–3939, 1998.
Kasper-Giebl, A., Kalina, M. F., and Puxbaum, H.: Scavenging ratios for sulfate, ammonium and nitrate determined at Mt. Sonnblick (3106 m a.s.l.), Atm. Env., 33, 895–906, 1999.
Kasper-Giebl, A., Koch, A., Hitzenberger, R., and Puxbaum, H.: Scavenging Efficiency of "Aerosol carbon" and Sulfate in Supercooled Clouds at Mt. Sonnblick (3106 m a.s.l., Austria), J. Atm. Chem., 35, 33–46, 2000.
Keene, W. C., Mosher, B. W., Jacob, D. J., Munger, J. W., Talbot, R. W., Artz, R. S., Maben, J. R., Daube, B. C., and Galloway, J. N.: Carboxylic acids in clouds at a high-elevation forested site in Central Virginia, J. Geophys. Res., 100, D5, 9345–9357, 1995.
Krämer, M., Schütz, L:, Elbert, W., and Beltz, N.: Cloud processing of continental aerosol particles: Experimental investigations for different drop sizes, J. Geophys. Res. 105, D9, 11739–11752, 2000.
Kruisz, C., Berner, A., and Branntner, B.: A cloud water sampler for high wind speeds, in: P.M.

Borell, P. Borell, T. Cvitas, W. Seiler (eds), Proc. EUROTRAC Symp. '92, SPB Academic Publishing bv, 523–525, The Hague, 1993.
Kulmala, M., Korhonen, P., Laaksonen, A., and Vesala, T.: Changes in cloud properties due to NO_x emissions, Geophys. Res. Lett., 22, 3, 239–242, 1995.
Laj, P., Flossmann, A. I., Wobrock, W., Fuzzi, S., Orsi, G., Ricci, L., Mertes, S., Schwarzenböck, A., Heintzenberg, J., and Ten Brink, H.: Behaviour of H_2O_2, NH_3, and black carbon in mixed-phase clouds during CIME, Atm. Res., 58, 4, 315–336, 2001.
Laj, P., Fuzzi, S., Lazzari, A., Ricci, L., Orsi, G., Berner, A., Schell, D., Günther, A., Wendisch, M., Wobrock, W., Frank, G., Martinsson, B., and Hillamo, R.: The size-dependent chemical composition of fog drops, Contr. Atmos. Phys., 71, 1, 115–130, 1998.
Laj, P., Fuzzi, S., Facchini, M. C., Lind, J. A., Orsi, G., Preiss, M., Maser, R., Jaeschke, W., Seyffer, E., Arends, B. G., Mols, J. J., Acker, K., Wieprecht, W., Moller, D., Colvile, R. N., Gallagher, M. W., Beswick, K. M., Hargreaves, K. J., Storeton-West, R. L., and Sutton, M. A.: Cloud processing of soluble gases, Atmospheric Environment, 31, 16, 2589–2598, 1997.
Lawrence, M. G. and Crutzen, P. J.: The impact of cloud particle gravitational settling on soluble trace gas distribution, Tellus, 50B, 3, 263–289, 1998.
Lelieveld, J. and Crutzen, P. J.: The role of clouds in tropospheric photochemistry, J. Atmos. Chem., 12, 229–267, 1991.
Limbeck, A. and Puxbaum, H.: Dependence of in-cloud scavenging of polar organic aerosol compounds on the water solubility, J. Geophys. Res., 105, D15, 19857–19867, 2000.
Marsh, A. R. W. and Mc Elroy, W. J.: The dissociation constant nad Henry's law constant of HCL in aqueous solution, Atm. Env., 19, 1075–1080, 1985.
Munger, J. W., Jacob, D. J., Daube, B. C., Horowitz, L. W., Keene, W. C., and Heikes, B. G.: Formaldehyde, glyoxal, and methylglyoxal in air and cloudwater at a rural mountain site in central Virginia, J. Geophys. Res., 100D, 9325–9333, 1995.
Neuman, J. A., Huey, L. G., Ryerson, T. B., and Fahey, D. W.: Study of inlet materials for sampling atmospheric nitric acid, Environ. Sci. Technol., 33, 1133–1136, 1999.
Noone, K. J., Ogren, J. A., Noone, K. B., Hallberg, A., Fuzzi, S., and Lind, J. A.: Measurements of the partitioning of hydrogen peroxide in a stratiform cloud, Tellus, 43B, 280–290, 1991.
Ogren, J. A. and Charlson, R. J.: Implications for models and measurements of chemical inhomogeneities among cloud droplets, Tellus, 44B, 208–225, 1992.
Ogren, J. A., Noone, K. J., Hallberg, A., Heintzenberg, J., Schell, D., Berner, A., Solly, I., Kruisz, C., Reischl, G., Arends, B. G., and Wobrock, W.: Measurements of the size dependence of

the concentration of non-volatile material in fog droplets, Tellus, 44B, 570–580, 1992.
Ogren, J.A., Heitzenberg, J., and Charlson, R. J.: In-situ sampling of clouds with a droplet to aerosol converter, Geophys. Res. Lett., 12, 121–24, 1985.
Pandis, S. N. and Seinfeld, J. H.: Should bulk cloudwater samples obey Henry's law?, J. Geophys. Res., 96D, 10791–10798, 1991.
Pruppacher, H. R. and Klett, J. D.: Microphysics of clouds and precipitation, Dordrecht, Reidel, 1997.
Rao, X. and Collett, J. L.: Behavior of S(IV) and formaldehyde in a chemically heterogeneous cloud, Environ. Sci. Technol., 29, 1023–1031, 1995.
Ricci, L., Fuzzi, S., Laj, P., Lazzari, A., Orsi, G., Berner, A., Günther, A., Arends, B., and Wendisch, M.: Gas/liquid equilibria in polluted fog, Contr. Atmos. Phys., 71, 1, 159–170, 1998.
Richards, L. W., Anderson, J. A., Blumenthal, D. L., McDonald, J. A., Kok, G. L., and Lazrus, A. L.: Hydrogen peroxide and sulfur (IV) in Los Angeles cloud water, Atmos. Envir., 17, 911–914, 1983.
Saxena, P. and Hildemann, L. M.: Water-soluble organics in atmospheric particles: A critical review of the literature and application of thermodynamics to identify candidate compounds, J. Atmos. Chem., 24, 57–109, 1996.
Schell, D., Wobrok, W., Maser, R., Preiss, M., Jaeschke, W., Georgii, H. W., Gallagher, M. W., Bower, K. N., Beswick, K. M., Pahl, S., Facchini, M. C., Fuzzi, S., Wiedensholer, A., Hansson, H. C., and Wendisch, M.: The size-dependent chemical composition of cloud droplets, Atmos. Envir., 1997.
Schwartz, S. E.: Mass-transport consideration pertinent to aqueous phase reactions of gases in liquid water clouds. Chemistry of the Atmospheric Multiphase Systems, W. Jaeschke, Heildelberg, Springer-Verlag, 451–471, 1986.
Sellegri, K., Laj, P., Peron, F., Dupuy, R., Legrand, M., Preunkert, S., Putaud, J.-P., Cachier, H., and Ghermandi, G.: Mass balance of winter time free tropospheric aerosol at the Puy de Dôme (France), J. Geophys. Res., 2003a.
Sellegri, K., Laj, P., Dupuy, R., Legrand, M., Preunkert, S., Putaud, J.-P., and Cachier, H.: size-dependent scavenging efficiencies of multi-component atmospheric aerosols in clouds, J. Geophys. Res., 2003b.
Talbot, R. W., Scheuer, E. M., Lefer, B. L., and Luke, W. T.: Measurements of sulfur dioxide during GASIE with the mist chamber technique, J. Geophys. Res., 102, 16,273–16,278,

1997.
Vocourt, V.: Etalonnage et Simulation numrique d'une Sonde à Impaction Virtuelle (CVI) dans le cadre de l'étude des propriétés physico-chimiques des particules nuageuses, these de doctorat, Clermont Ferrand, Université Blaise Pascal, 2002.
Voisin, D., Legrand, M. and Chaumerliac, N.: Scavenging of acidic gases (HCOOH, CH_3COOH, HNO_3, HCl, and SO_2) and ammonia in mixed liquid-solid water clouds at the Puy de Dôme mountain, J. Geophys. Res., 105, D5, 6817–6836, 2000.
Warneck, P.: The equilibrium distribution of atmospheric gases between the two phases of liquid water clouds, Chemistry of Multiphase Atmospheric Systems, W. Jaeschke, Heidelberg, Springer-Verlag, 1986.
Weast, R. C.: Handbook of Chemistry and Physics, Boca Raton, Florida, 1984.
Winiwarter, W., Brantner, B., and Puxbaum, H.: Comments on: Should bulk cloudwater or fogwater samples obey Henry's law?, J. Geophys. Res., 97D, 6075–6078, 1992.
Winiwarter, W., Fierlinger, H., Puxbaum, H., Facchini, M. C., Arends, B. G., Fuzzi, S., Schell, D., Kaminski, U., Pahl, S., Schneider, T., Berner, A., Solly, I., and Kruisz, C.: Henry's law and the behaviour of weak acids and bases in fog and cloud, J. Atmos. Chem., 19, 173–188, 1994.
Winiwarter, W., Puxbaum, H., Facchini, M. C., Orsi, G., Beltz, N., Enderle, K., and Jaeschke, W.: Organic acid gas and liquid phase measurements in Po Valley autumn-winter conditions in the presence of fog, Tellus, 40B, 348–357, 1988.
Wobrock, W., Flossmann, A. I., Monier, M., Pichon, J.-M., Cortez, L., Fournol, J.-F., Schwarzenböck, A., Mertes, S., Heintzenberg, J., Laj, P., Orsi, G., Ricci, L., Fuzzi, S., Ten Brink, H., Jongejan, P., and Otjes, R.: The Cloud Ice Mountain Experiment (CIME) 1998: experiment overview and modelling of the microphysical processes during the seeding by isentropic gas expansion, Atm. Res., 58, 231–265, 2001.
Wobrock, W., Schell, D., Maser, R., Jaeschke, W., Georgii, H.-W., Wieprecht, W., Arends, B. G., Mls, J. J., Kos, G. P. A., Fuzzi, S., Facchini, M. C., Orsi, G., Berner, A., Solly, I., Kruisz, C., Svenningsson, I. B., Wiedensohler, A., Hansson, H.-C., Ogren, J. A., Noone, K. J., Hallberg, A., Pahl, S., Schneider, T., Winkler, P., Winiwarter, W., Colvile, R. N., Choularton, T. W., Flossmann, A. I., and Borrmann, S.: The Kleiner Feldberg Cloud Experiment 1990, An overview, J. Atmos. Chem. 19, 3–35, 1994.
Zhang, M. H. and Mc Murry, H.: Evaporative losses of fine particulate nitrates during sampling, Atmos. Env., 26A, 18, 3305–3312, 1992.

Table 1. Sampling conditions. All cloud water samples were taken during super-cooled conditions. Variabilily is calculated as standard deviations amongst samples of a cloud event

Impact sample	Date/ hour	Number of CDI samples	Number of MC samples	Mean LWC (g m^{-3})	Temperature K	Average H+ converted to ph (CDI)
	12/02 22:10					
1		9	6	0.37 ± 0.17	272,7 ± 1.2	4.4 ± 0.5
	14/02 10:00					
	17/02 12:40					
2		11	2	0.44 ± 0.09	268.2 ± 0.6	4.2 ± 0.6
	18/02 10:00					
	22/02 15:36					
3		10	4	0.29 ± 0.08	271.8 ± 1.05	5.2 ± 0.9
	23/02 11:45					
	23/02 15:20					
4		8	1	0.27 ± 0.05	270.3 ± 2.1	3.7 ± 0.2
	24/02 02:06					
	28/02 00:15					
5		10	3	0.15 ± 0.06	267.4 ± 0.3	4.2 ± 0.3
	01/03 10:00					

ACPD
3, 479–519, 2003

Table 2. Atmospheric detection limits for a typical 25 m^3 sample for impactor data, for a typical 0.3 g m^{-3} LWC for CDI data; and for a typical one hour long sampling time for MC data

Nmol m^{-3}	Ace	For	HCl/Cl^-	$H\,NO_3/NO_3^-$	SO_4^{2-}	Ox	NH_3/NH_4^+
Aerosol	0.029	0.018	0.106	0.027	0.027	0.003	0.048
Liquid	0.053	0.080	0.16	0.24	0.33	0.014	0.46
Gaz	0.46	0.71	2.3	0.44	1.2	0.35	5.3

ACPD
3, 479–519, 2003

Table 3. Atmospheric concentration (in nmol m^{-3}) in the liquid phase of clouds measured with the CDI. Samples are averaged over the entire period of the cloud event and corrected for LWC to convert from ng l^{-1} to nmol m^{-3}

Event	CH_3COO^-	$HCOO^-$	Cl^-	NO_3^-	SO_4^{2-}	$C_2O_4^{2-}$	NH_4^+	NH_4^+/SO_4^{2-}	NO_3^-/SO_4^{2-}
1	0.97	1.1	5.9	10.4	3.1	0.18	11.6	0.9	0.9
2	2.2	2.3	9.3	85.6	20.4	0.65	62.5	0.8	1.1
3	0.62	0.64	0.44	4.0	1.1	0.13	7.4	1.8	1.0
4	1.7	1.8	7.8	13.9	6.2	0.26	20.3	0.8	0.6
5	1.5	1.0	4.0	14.3	5.2	0.25	14.3	0.7	0.7

Table 4. Atmospheric concentrations in particulate residual aerosol, in nmol m^{-3}

Event	CH_3COO^-	$HCOO^-$	Cl^-	NO_3^-	SO_4^{2-}	$C_2O_4^{2-}$	NH_4^+	NH_4^+/SO_4^{2-}	NO_3^-/SO_4^{2-}
1	<dl	0.02	0.43	6.0	1.9	0.07	5.9	0.8	0.8
2	0.10	0.17	0.86	26.3	12.4	0.20	26.2	0.6	0.6
3	<dl	<dl	0.51	3.5	0.88	0.09	6.0	1.7	1.0
4	0.03	<dl	3.3	8.0	3.4	0.11	12.1	0.9	0.6
5	0.03	0.03	0.51	4.7	3.2	0.08	7.4	0.6	0.4

ACPD
3, 479–519, 2003

Table 5. Concentration of gaseous species (in nmol m^{-3}) in the interstitial phase of clouds

Event	CH_3COOH	HCOOH	HCl	HNO_3	SO_2	$H_2C_2O_4$	NH_3
1	11	5.8	5.7	0.74	<dl (0.60)	<dl (0.28)	18
2	17	7.0	<dl (0.74)	<dl (0.39)	<dl (0.6)	<dl (0.16)	39
3	7.6	3.9	<dl (0.14)	<dl (0.35)	<dl (0.29)	<dl (0.18)	52
4	10	5.5	<dl (0.46)	<dl (0.32)	<dl (0.0)	<dl (0.03)	33
5	6.0	2.8	<dl (0.74)	1.9	1.5	<dl (0.11)	27
PDD2000	13	4.7	14	0.00	0.67		26
PDD1998 Voisin et al. (2000)	13±7	14±8	2.7±2.6	6.9±6.0	18±14		8±7

Table 6. Concentrations of particulate aerosols (in nmol m^{-3}), in the interstitial phase of clouds

Event	CH_3COO^-	$HCOO^-$	Cl^-	NO_3^-	SO_4^{2-}	$C_2O_4^{2-}$	NH_4^+	NH_4^+/SO_4^{2-}	NO_3^-/SO_4^{2-}
1	<dl (0.007)	<dl (0.01)	<dl (0.02)	0.61	0.52	0.05	1.3	0.7	0.3
2	<dl (0.010)	0	0.14	1.7	1.2	0.07	4.2	0.9	0.4
3	<dl (0)	0.08	<dl (0.01)	0.68	=dl	0.05	1.1	0.9	–
4	0.032	<dl (0)	0.36	1.32	1.1	0.09	3.4	0.8	0.3
5	<dl (0.014)	0.24	0.17	1.0	0.47	0.09	1.0	0.6	0.6

ACPD
3, 479–519, 2003

Table 7. Solubilisation and dissociation constants used in the calculations of the Henry's equilibrium shown in Table 8. (1) Marsh and Mc Elroy (1985), (2) Jacob (1986), (3) Graedel and Goldberg (1983), (4) Chameides (1984), (5) Saxena and Hildemann (1996), (6) Weast (1984)

Solubilisation	K_H (298) $Mol.l^{-1}.atm^{-1}$	$\Delta H/R$ K	Ref
$HCL(g) \leftrightharpoons HCl(l)$	1.1	−2023	(1)
$HCOOH(g) \leftrightharpoons HCOOH(l)$	$3.7\ 10^3$	−5700	(2)
$CH_3COOH(g) \leftrightharpoons CH_3COOH(l)$	$5.0\ 10^3$	−5890	(3)
$HNO_3 \leftrightharpoons HNO_3(l)$	$1.5\ 10^5$	−8700	(2)
$SO_2 \leftrightharpoons SO_2(l)$	1.23	−3120	(4)
$H_2C_2O_4(g) \leftrightharpoons H_2C_2O_4(l)$	$5\ 10^8$	–	(5)
$NH_3 \leftrightharpoons NH_4(l)$	58	−4085	(1)
Dissociations	K_A (298) $Mol.l^{-1}.atm^{-1}$	$\Delta H/R$ K	Ref
$HCL \leftrightharpoons H^+ + Cl^-$	$1.7\ 10^6$	−6889	(1)
$HCOOH \leftrightharpoons HCOO^- + H^+$	$1.8\ 10^{-4}$	−150	(4)
$CH_3COOH \leftrightharpoons CH_3COO^- + H^+$	$1.8\ 10^{-5}$	−46	(4)
$HNO_3 \leftrightharpoons NO_3^- + H^+$	22	–	(4)
$SO_2 + H_2O \leftrightharpoons HSO_3^- + H^+$	$1.7\ 10^{-2}$	−2090	(4)
$HSO_3^- \leftrightharpoons SO_3^{2-} + H^+$	$6.3\ 10^{-8}$	−1510	(4)
$H_2C_2O_4 \leftrightharpoons H_2C_2O_4^- + H^+$	$5.9\ 10^{-2}$	–	(6)
$HC_2O_4^- \leftrightharpoons C_2O_4^{2-} + H^+$	$6.4\ 10^{-5}$	–	(6)
$NH_3 + H_2O \leftrightharpoons NH_4^+ + OH^-$	$1.7\ 10^{-5}$	−4325	(1)

ACPD
3, 479–519, 2003

Table 8. Liquid/total fractions R_x (%) calculated from MC and CDI mean concentrations labeled as "m", compared to theoretical liquid/total fractions labeled as "th", calculated as $H^*/(1+H^*)$. Ranges are used for measured contributions when gas concentrations are below dl : the R_x higher limit is calculated for $[X]_{gas}$ = dl

Event	CH_3COO^-		$HCOO^-$		Cl^-		NO_3^-		SO_4^{2-}		$C_2O_4^{2-}$		NH_4^+	
	m	th	m	th	m	th	m	th	m	th	m	th	m	th
1	8	16	16	20	51	100	93	100	84–100	0.5	39–100	100	39	100
2	11	32	25	28	93–100	100	100	100	97–100	0.3	80–100	100	62	100
3	8	52	14	80	75–100	100	92–100	100	78–100	15	41–100	100	12	100
4	14	40	24	59	94–100	100	98–100	100	100	10	88–100	100	38	100
5	20	11	27	10	84–100	100	89	100	77	0.1	69–100	100	35	100
median	11	32	24	28	84–100	100	93–100	100	84–100	0.5	69–100	100	38	100
Voisin et al. (2000)	10		10		80		90						90	
Kasper and Puxbaum (1998)							39		54				56	

Table 9. Lower limit of the gaseous contribution to the concentration of cloud droplets, calculated from the CDI and CVI data (%) in absolute (Abs) as (CDI-CVI)/CDI and in relative (/Na) as (CDI_{Na}-CVI_{Na})/CDI_{Na}

Event	CH_3COO^-		$HCOO^-$		Cl^-		NO_3^-		SO_4^{2-}		$C_2O_4^{2-}$		NH_4^+	
	Abs	/Na	Abs	/Na	Abs	/Na	Abs	/Na	Abs	/Na	Abs	/Na	Abs	/Na
1	98	95	98	95	93	81	42		40		63		49	
2	95	94	93	90	91	87	69	58	39	16	70	58	58	42
3	97	99	97	98		43	12	57	18	59	32	66	19	60
4	98	98	99	99		67	43	56	45	58	56	66	40	54
5	98	98	97	98	87	91	67	78	38	58	68	78	48	65
Median	97,7	98,4	96,8	97,8	90,8	80,8	42,6	57,2	39,4	57,6	63,0	66,2	48,4	57,2

ACPD
3, 479–519, 2003

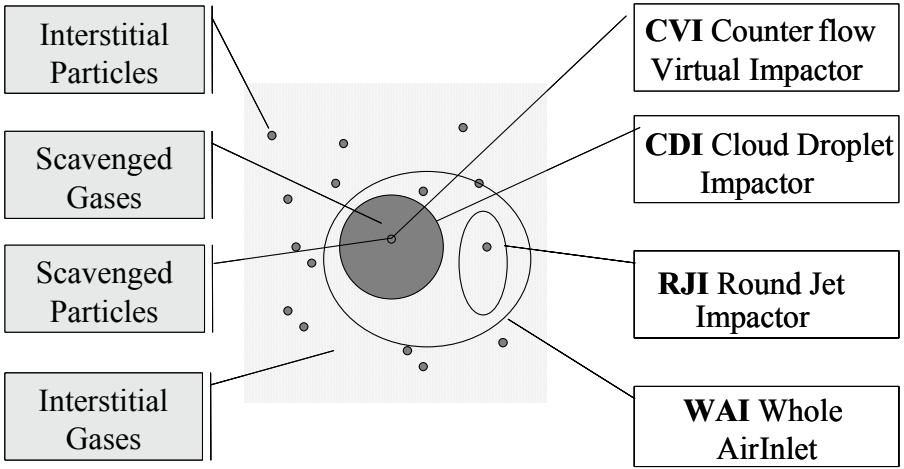

Fig. 1. Experimental devices (right labels) used in sampling the different cloud reservoirs (left labels).

ACPD
3, 479–519, 2003

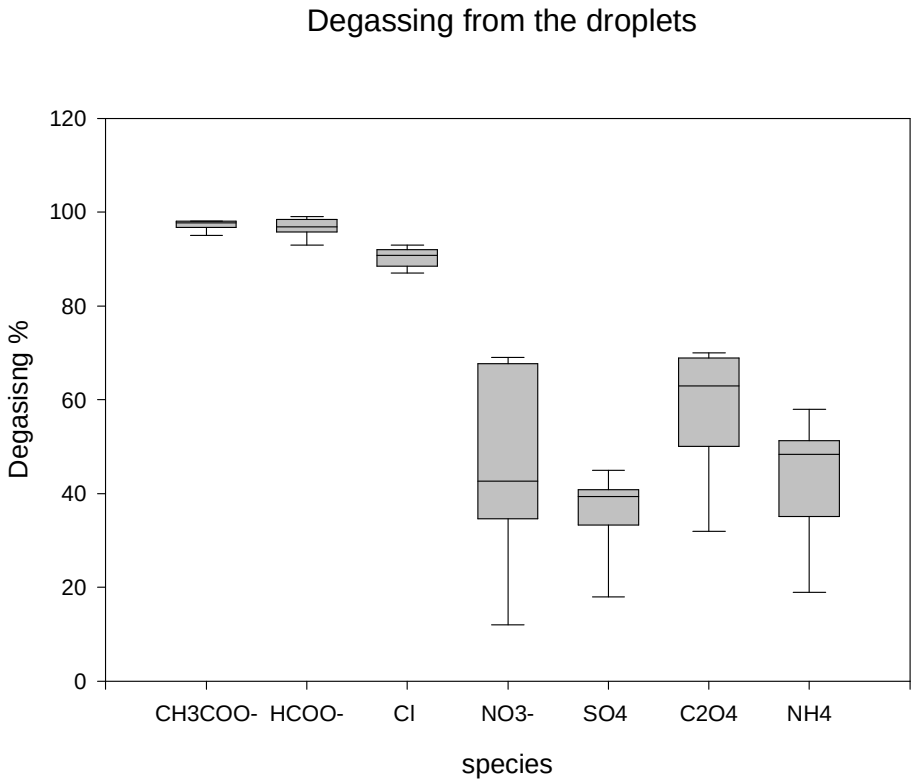

Fig. 2. Percentages of degassing mass from the droplets when evaporating, calculated as $([X]_{CDI} - [X]_{CVI})/[X]_{CDI}$.

ACPD
3, 479–519, 2003

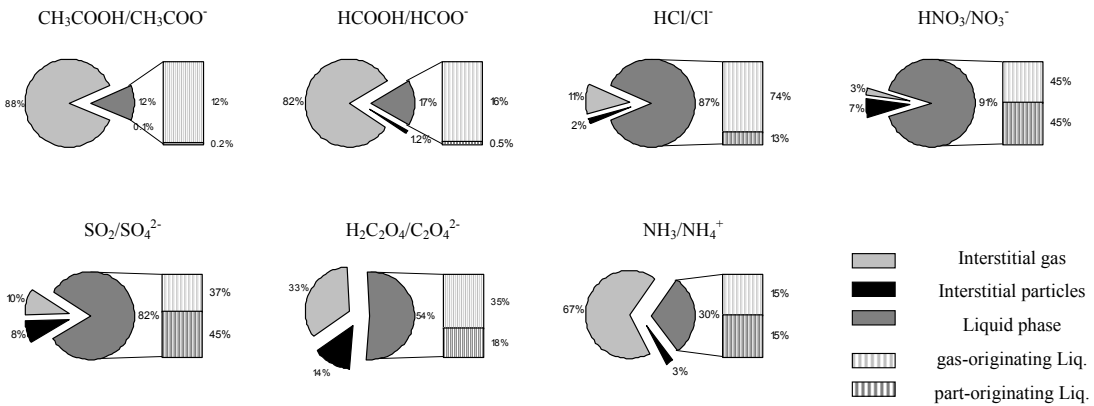

Fig. 3. Phase partitioning between the gas, particulate and liquid phases in cloud calculated from concentrations from the RJI+Cascade Impactor (particulate), RJI+Mist chambers (interstitial gaz phase) and CDI (liquid phase). Further partitioning within the liquid phase between the gas-originating fraction and the particle-originating fraction are calculated from the CVI/CDI comparison. Gas concentrations are below detection limits for HCL, HNO_3, SO_2 and $H_2C_2O_4$, and thus their concentration are assimilated to detection limits.

ACPD
3, 479–519, 2003